JOC*Article*

Synthesis and Optical Properties of Isomeric Branched π-Conjugated Systems

Jean-François Nierengarten,* Sheng Zhang, Aline Gégout, and Maxence Urbani

Groupe de Chimie des Fullerènes et des Systèmes Conjugués, Ecole Européenne de Chimie, Polymères et Matériaux (ECPM), Université Louis Pasteur et CNRS, 25 rue Becquerel, 67087 Strasbourg Cedex 2, France

Nicola Armaroli,* Giancarlo Marconi, and Yannick Rio

Istituto per la Sintesi Organica e la Fotoreattività, Molecular Photoscience Group, Consiglio Nazionale delle Ricerche, via Gobetti 101, 40129, Bologna, Italy

jfnierengarten@chimie.u-strasbg.fr; armaroli@isof.cnr.it

Received April 4, 2005

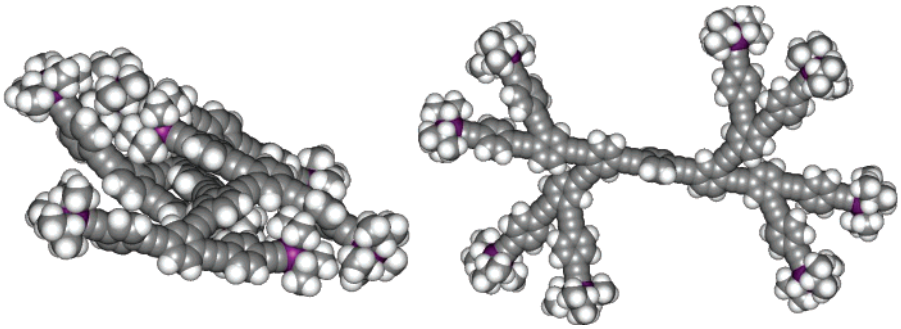

Branched conjugated systems with a terminal alkyne function have been prepared starting from 4-(triisopropylsilylethynyl) phenylacetylene by applying the following iterative reaction sequence: (i) metal-catalyzed cross-coupling reaction of the terminal alkyne with 3,4-dibromobenzaldehyde or 2,5- dibromobenzaldehyde; (ii) Corey−Fuchs dibromoolefination and treatment with an excess of LDA. The building blocks thus prepared have been subjected to a Pd-catalyzed cross-coupling reaction with 1,4-diiodobenzene to yield isomeric branched π-conjugated systems containing 7 (first generation) or 15 (second generation) phenyl units connected by ethynyl spacers. The different π-conjugation patterns in those isomeric derivatives have a dramatic effect on their electronic properties, as attested by the differences observed in their absorption and emission spectra. Finally, theoretical calculations have been performed to rationalize the optical properties of these compounds.

Introduction

The past several years have seen a considerable interest in the synthesis of new linear monodisperse π-conjugated oligomers.[1,2] Whereas the initial driving force for the synthesis and the study of well-defined oligomers was the development of structure−property relationships to rationalize the properties of the corresponding π-conjugated polymers, this research has evolved into an independent field of its own.[1,2] Its development has generated some spectacular molecular architectures with high potential for optoelectronic applications.[1−3] This has given impetus to make this research a truly interdisciplinary branch of science located at the interfaces between chemistry, physics, and materials science. It must also be added here that the bottom-up approach for the construction of electronic circuitry starting from nanometer-sized π-conjugated molecular nanowires is

(1) Müllen, K.; Wegner, G. *Electronic Materials: The Oligomer Approach*; Wiley-VCH: Weinheim, 1998.

(2) (a) Tour, J. M. *Chem. Rev*. **1996**, *96*, 537. (b) Martin R. E., Diederich, F. *Angew. Chem., Int. Ed.* **1999**, *38*, 1350. (c) Roncali, J. *Acc. Chem. Res.* **2000**, *33*, 147. (d) Tour, J. M. *Acc. Chem. Res.* **2000**, *33*, 791. (e) Diederich, F. *Chem. Commun*. **2001**, 219. (f) Segura, J. L.; Martin, N. *J. Mater. Chem*. **2000**, *10*, 2403.

(3) (a) Kraft, A.; Grimsdale, A. C.; Holmes, A. B. *Angew. Chem., Int. Ed*. **1998**, *37*, 403. (b) Bernius, M. T.; Inbasekaran, M.; O'Brian, J.; Wu, W. *Adv. Mater*. **2000**, *12*, 1737. (c) Mitshke, U.; Bäuerle, P. *J. Mater. Chem.* **2000**, *10*, 1471. (d) Sano, T.; Nishio, Y.; Hamada, Y.; Takahashi, H.; Usuki, T.; Shibata, K. *J. Mater. Chem*. **2000**, *10*, 157. (e) Shirota, Y. *J. Mater. Chem*. **2000**, *10*, 1. (f) Nalva, H. S. *Adv. Mater*. **1993**, *5*, 341. (g) Marks, T. J.; Ratner, M. A. *Angew. Chem., Int. Ed*. **1995**, *34*, 155. (h) Nierengarten, J.-F. *Sol. Energy Mater. Sol. Cells* **2004**, *83*, 187.

10.1021/jo0506581 CCC: $30.25
Published on Web 08/13/2005

CHART 1

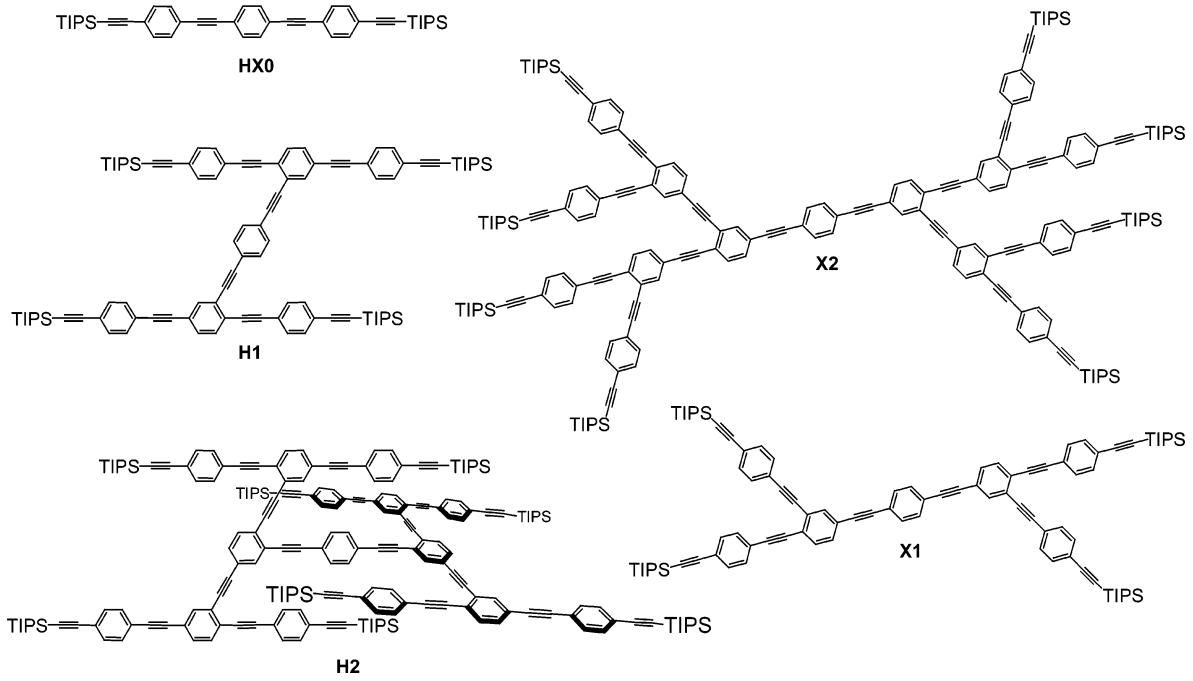

particularly appealing and gives rise to tremendous research efforts nowadays.[4]

The rapid progress achieved in the synthesis of monodisperse π-conjugated oligomers has also stimulated the development of other fascinating families of compounds. These novel molecules include macrocyclic π-systems,[5] substructures of new graphite-like two-dimensional networks,[5] fullerene-like three-dimensional cages,[5] and hyperbranched structures.[6−8] As far as conjugated dendrimers are concerned, almost all of the systems described so far have been constructed from symmetrical building blocks based on 1,3,5-trisubstituted phenyl rings.[7,8] As a result of the *meta*-branching scheme, the π-conjugation of these dendritic molecules is, however, rather limited. More recently, Peng and co-workers have reported the preparation of new conjugated dendrimers based on 1,2,4-trisubstituted phenyl units in which the different branches exhibit different conjugation lengths.[9] Indeed, the unsymmetric substitution on the aromatic ring produces *para*-linked phenylacetylene units allowing an increase of the conjugation length when the dendritic generation is increased. By following a similar approach, we now report the synthesis of the isomeric branched π-conjugated systems **H1**−**2** and **X1**−**2** (Chart 1). Whereas **X1** and **X2** are similar to the dendritic systems reported by Peng and co-workers, compounds **H1** and **H2** have unprecedented structural features. To understand the influence of the conjugation pathways within these isomeric systems, the excited-state properties of **H1**−**2** and **X1**−**2** have been investigated and compared to those of the corresponding model compound **HX0**.

Results and Discussion

Synthesis. The preparation of **HX0** is depicted in Scheme 1. 4-Bromobenzaldehyde (**1**) was subjected to a Pd-catalyzed cross-coupling reaction[10] with triisopropylsilylacetylene to give **2** in 98% yield. Subsequent treatment with $CBr_4/PPh_3/Zn$ under the conditions described by Corey−Fuchs[11] yielded dibromoolefine **3** in 99% yield. Elimination of HBr and halogen−metal exchange was best achieved with an excess of LDA[12] in THF at −78 °C, and the resulting anion was quenched with NH_4Cl to give monoprotected bisalkyne **4** in 90% yield. The OPE trimer **HX0** was then obtained in 84% yield by Pd-

(4) (a) Kovtyukhova, N. I.; Mallouk, T. E. *Chem. Eur. J*. **2002**, *8*, 4355. (b) Carroll, R. L.; Gorman, C. B. *Angew. Chem., Int. Ed*. **2002**, *41*, 4379. (c) Balzani, V.; Credi, A.; Venturi, B. *Chem. Eur. J*. **2002**, *8*, 5525.

(5) (a) Diederich, F.; Rubin, Y. *Angew. Chem., Int. Ed. Engl*. **1992**, *31*, 1101. (b) Diederich, F. *Nature* **1994**, *369*, 199. (c) Haley, M. M. *Synlett* **1998**, 557. (d) Bunz, U. H. F.; Rubin, Y.; Tobe, Y. *Chem. Soc. Rev*. **1999**, *28*, 107. (e) Watson, M. D.; Fechtenkötter, A.; Müllen, K. *Chem. Rev*. **2001**, *101*, 1267.

(6) Newkome, G. R.; Moorefield, C. N.; Vögtle, F. *Dendrimers and Dendrons: Concepts, Syntheses, Applications*; VCH: Weinheim, 2001.

(7) (a) Moore, J. S.; Xu, Z. *Polym. Prep.* **1991**, *32*, 629. (b) Moore, J. S.; Xu, Z. *Macromolecules* **1991**, *24*, 5893. (c) Moore, J. S.; Xu, Z. *J. Am. Chem. Soc*. **1994**, *116*, 4537. (d) Pesak, D. J.; Moore, J. S. *Angew. Chem., Int. Ed*. **1997**, *36*, 1636. (e) Moore, J. S.; Xu, Z. *Angew. Chem., Int. Ed. Engl*. **1993**, *32*, 246. (e) Moore, J. S. *Acc. Chem. Res*. **1997**, *30*, 402. (f) Devadoss, C.; Bharathi, P.; Moore, J. S. *J. Am. Chem. Soc*. **1996**, *118*, 9635.

(8) (a) Deb, S. K.; Maddux, T. M.; Yu, L. *J. Am. Chem. Soc*. **1997**, *119*, 9079. (b) Meier, H.; Lehmann, M. *Angew. Chem., Int. Ed*. **1998**, *37*, 643. (c) Lehmann, M.; Schartel, B.; Hennecke, M.; Meier, H. *Tetrahedron* **1999**, *55*, 13377. (d) Meier, H.; Lehmann, M.; Kolb, U. *Chem. Eur. J*. **2000**, *6*, 2462. (e) Diez-Barra, E.; Garcia-Martinez, J. C.; Rodriguez-Lopez, J. *Tetrahedron Lett*. **1999**, *40*, 8181. (f) Diez-Barra, Garcia-Martinez, J. C.; Rodriguez-Lopez, J.; Gomez, R.; Segura, J. L.; Martin, N. *Org. Lett*. **2000**, *2*, 3651. (g) Accorsi, G.; Armaroli, N.; Eckert, J.-F.; Nierengarten, J.-F. *Tetrahedron Lett*. **2002**, *43*, 65. (h) Segura, J. L.; Gomez, R.; Martin, N.; Luo, C. P.; Swartz, A.; Guldi, D. M. *Chem. Commun*. **2001**, 707. (i) Guldi, D. M.; Swartz, A.; Luo, C.; Gomez, R.; Segura, J. L.; Martin, N. *J. Am. Chem. Soc*. **2002**, *124*, 1087. (j) Langa, F.; Gomez-Escalonilla, M. J.; Diez-Barra, E.; Garcia-Martinez, J. C.; de la Hoz, A.; Rodriguez-Lopez, J.; Gonzalez-Cortes, A.; Lopez-Arza, V. *Tetrahedron Lett*. **2001**, *42*, 3435.

(9) (a) Peng, Z.; Pan, Y.; Xu, B.; Zhang, J. *J. Am. Chem. Soc*. **2000**, *122*, 6619. (b) Pan, Y.; Lu, M.; Peng, Z.; Melinger, J. S. *J. Org. Chem*. **2003**, *68*, 6952.

(10) (a) Takahashi, S.; Kuroyama, Y.; Sonogashira, K.; Nagihara, N. *Synthesis* **1980**, 627. (b) *Metal-Catalyzed Cross-Coupling Reactions*; Diederich, F., Stang, P. J., Eds.; Wiley-VCH: Weinheim, 1998.

(11) Corey, E. J.; Fuchs, P. L. *Tetrahedron Lett*. **1972**, *13*, 3769.

SCHEME 1[a]

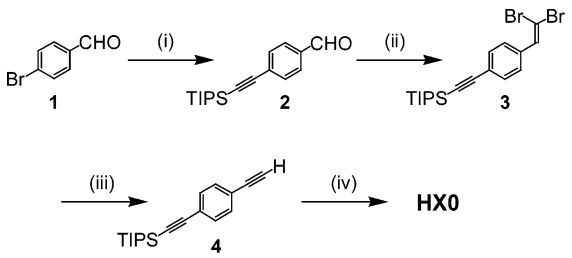

[a] Reagents and conditions: (i) triisopropylsilylacetylene, $PdCl_2(PPh_3)_2$, CuI, PPh_3, Et_3N, THF (98%); (ii) CBr_4, PPh_3, Zn dust, CH_2Cl_2 (99%); (iii) LDA, THF then NH_4Cl, H_2O (90%); (iv) 1,4-diiodobenzene, $PdCl_2(PPh_3)_2$, CuI, PPh_3, Et_3N, THF (84%).

SCHEME 2[a]

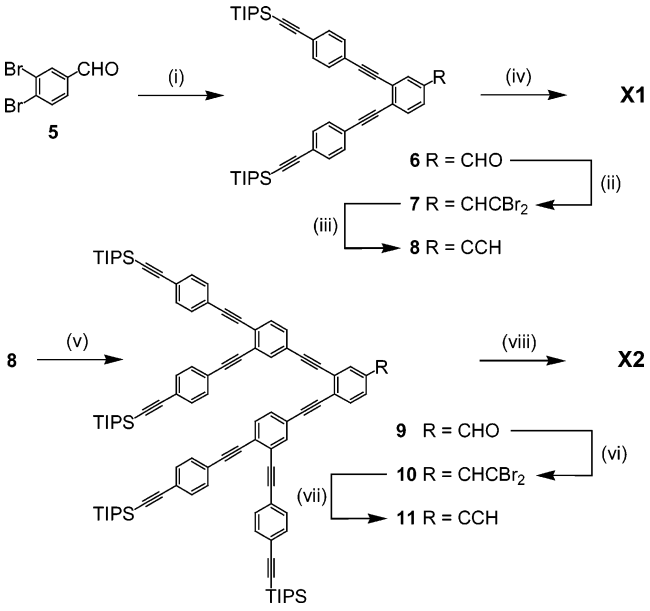

[a] Reagents and conditions: (i) **4**, $PdCl_2(PPh_3)_2$, CuI, PPh_3, Et_3N, THF (75%); (ii) CBr_4, PPh_3, Zn dust, CH_2Cl_2 (95%); (iii) LDA, THF then NH_4Cl, H_2O (92%); (iv) 1,4-diiodobenzene, $PdCl_2(PPh_3)_2$, CuI, PPh_3, Et_3N, THF (81%); (v) **5**, $PdCl_2(PPh_3)_2$, CuI, PPh_3, Et_3N, THF (78%); (vi) CBr_4, PPh_3, Zn dust, CH_2Cl_2 (94%); (vii) LDA, THF then NH_4Cl, H_2O (94%); (viii) 1,4-diiodobenzene, $PdCl_2(PPh_3)_2$, CuI, PPh_3, Et_3N, THF (88%).

catalyzed cross-coupling between **4** and 1,4-diiodobenzene. Compound **HX0** was characterized by ^1H and ^{13}C NMR, UV−vis, and IR spectroscopies. In addition, the structure of **HX0** was confirmed by FAB mass spectrometry.

The synthesis of **X1**−**2** is shown in Scheme 2. Reaction of 3,4-dibromobenzaldehyde (**5**) with monoprotected bis-alkyne **4** under Sonogashira conditions gave the fist generation dendron **6** in 75% yield. Dibromoolefination according to Corey−Fuchs then provided **7**, which after treatment with an excess of LDA in THF at −78 °C and quenching with NH_4Cl afforded terminal alkyne **8**. Compound **8** was subjected to a Pd-catalyzed cross-coupling reaction with **5** to yield the second generation dendron **9**. Treatment with CBr_4/PPh_3/Zn and subsequent reaction of the resulting intermediate **10** with an excess of LDA yielded terminal alkyne **11**. Owing to the presence of the triisopropylsilyl (TIPS) substituents, dendrons **6**−**11** are highly soluble in common organic solvents (CH_2Cl_2, $CHCl_3$, THF), and ^1H and ^{13}C NMR characterization was easily achieved. As typical examples, the ^1H NMR spectra of compounds **6** and **9** recorded in $CDCl_3$ are shown in Figure 1. For both **6** and **9**, the resonance arising from the aldehydic proton is observed at ca. 10 ppm. In the aromatic region, the spectrum of **6** shows three sets of signals in a typical pattern for a 3,4-disubstituted benzaldehyde moiety as well as a pseudo-singlet at 7.50 ppm for the protons of the two *para*-disubstituted phenyl groups. The ^1H NMR of **9** is also consistent with the proposed structure. In addition to the signals corresponding to the protons of the central 3,4-diethynylbenzaldehyde moiety, the resonances arising from the two 1,3,4-triethynylbenzene units appear as a single set of three signals. These two aromatic rings are in principle nonequivalent; however, both benzene rings are substituted by three alkyne groups and must be in a similar chemical environment and are therefore pseudo-equivalent. Finally, the peaks of the peripheral *p*-diethynyl phenyl moieties appear between 7.44 and 7.47 ppm.

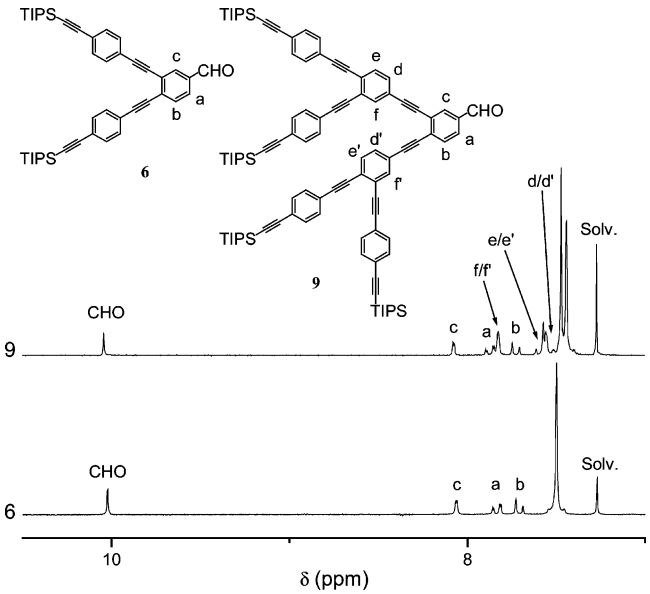

FIGURE 1. ^1H NMR spectra (300 MHz, $CDCl_3$) of compounds **6** (bottom) and **9** (top).

Compounds **6**−**11** were further characterized by IR spectroscopy. For all the derivatives, the characteristic C≡C stretching band is observed at 2151−2152 cm^{-1}. In the IR spectrum of **6** and **9**, the diagnostic aldehyde band is observed at ca. 1700 cm^{-1}. In the case of **8** and **11**, the C−H stretching band characteristic of the terminal alkyne function is seen at ca. 3300 cm^{-1}.

Compounds **15** and **18**, the key building blocks for the synthesis of **H1** and **H2**, respectively, were obtained from 2,5-dibromobenzaldehyde (**12**) by following a similar synthetic approach as the one described above for the preparation of the corresponding isomers **8** and **11** (Scheme 3). Pd-catalyzed cross-coupling reaction of terminal alkyne **4** with 2,5-dibromobenzaldehyde (**12**),

(12) (a) Nierengarten, J.-F.; Schreiber, M.; Diederich, F.; Gramlich, V. *New J. Chem*. **1996**, *20*, 1273−1284. (b) Solladié, N.; Gross, M. *Tetrahedron Lett*. **1999**, *40*, 3359. (c) Nierengarten, J.-F.; Gu, T.; Hadziioannou, G.; Tsamouras, D.; Krasnikov, V. *Helv. Chim. Acta* **2004**, *87*, 2948.

SCHEME 3[a]

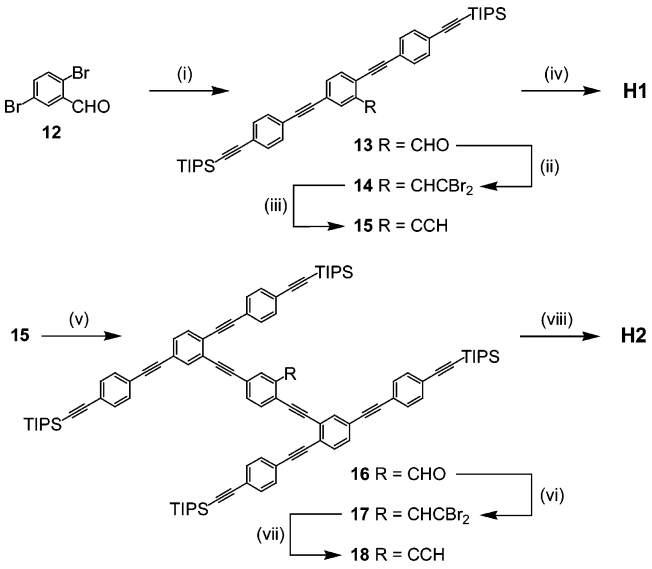

[a] Reagents and conditions: (i) **4**, $PdCl_2(PPh_3)_2$, CuI, PPh_3, Et_3N, THF (76%); (ii) CBr_4, PPh_3, Zn dust, CH_2Cl_2 (94%); (iii) LDA, THF then NH_4Cl, H_2O (96%); (iv) 1,4-diiodobenzene, $PdCl_2(PPh_3)_2$, CuI, PPh_3, Et_3N, THF (85%); (v) **12**, $PdCl_2(PPh_3)_2$, CuI, Et_3N (81%); (vi) CBr_4, PPh_3, Zn dust, CH_2Cl_2 (86%); (vii) LDA, THF then NH_4Cl, H_2O (87%); (viii) 1,4-diiodobenzene, $PdCl_2(PPh_3)_2$, CuI, PPh_3, Et_3N, THF (76%).

Corey−Fuchs dibromoolefination, and treatment with an excess of LDA gave **15** in an overall 69% yield. Subsequent Sonogashira coupling with **12** and treatment of the resulting **16** with CBr_4/PPh_3/Zn followed by reaction with an excess of LDA yielded terminal alkyne **18**.

The branched π-conjugated systems **H1**−**2** and **X1**−**2** were finally obtained by reaction of 1,4-diiodobenzene with an excess of the appropriate terminal alkyne precursor in the presence of $PdCl_2(PPh_3)_2$, CuI, and PPh_3 in Et_3N/THF (Schemes 2 and 3). In addition to the desired compounds, byproducts resulting from the homocoupling of the alkyne precursors were also formed under these conditions. However, the desired products were easily purified by column chromatography on silica gel, and **H1**−**2** and **X1**−**2** were isolated in good yields. Compounds **H1**−**2** and **X1**−**2** are well-soluble in common organic solvents such as CH_2Cl_2, $CHCl_3$, or THF, and complete spectroscopic characterization was easily achieved. Both ^1H and ^{13}C NMR spectra are in full agreement with the centrosymmetric structures of **H1**−**2** and **X1**−**2**. The ^1H NMR spectra of **H1** and **H2** recorded in $CDCl_3$ are shown in Figure 2.

In the aromatic region, the ^1H NMR spectrum of **H1** is characterized by a singlet for the aromatic protons of the central phenyl ring (H_a), three sets of signals for the 1,3,4-trisubstituted phenyl ring (H_b, H_c, and H_d), and a pseudo-singlet for the protons of the four *para*-disubstituted phenyl groups. The ^1H NMR of compound **H2** is also in full agreement with the proposed structure. The resonances arising from the three different pairs of equivalent 1,3,4-triethynylbenzene moieties are observed; in particular, H_b, H_e, and H_h give rise to three distinguishable signals in the expected 2:2:2 ratio. Three sets of pseudo-singlets are seen at 7.49, 7.40, and 7.39 for the peripheral *para*-disubstituted phenyl groups. Finally, the singlet corresponding to the protons of the central

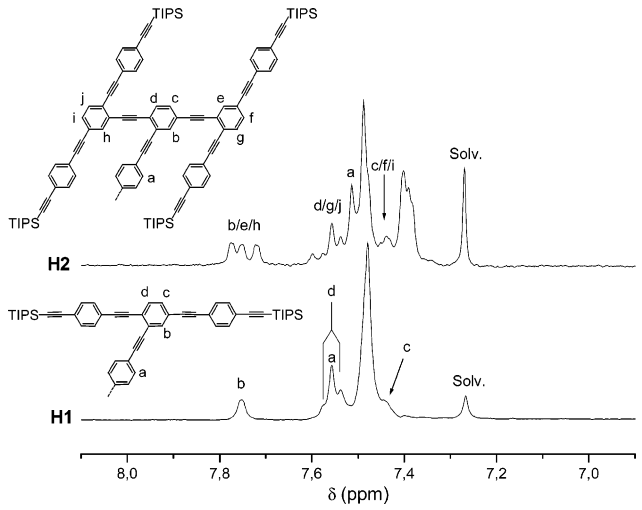

FIGURE 2. ^1H NMR spectra (300 MHz, $CDCl_3$) of compounds **H1** (bottom) and **H2** (top).

CHART 2

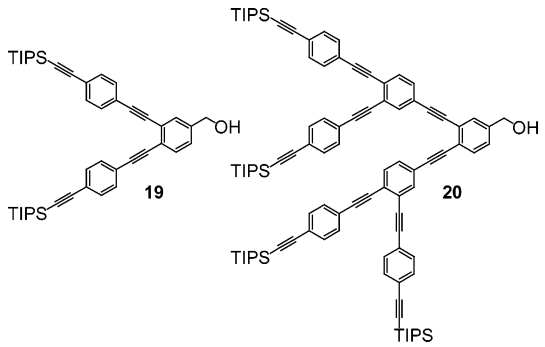

aromatic unit (H_a) is observed at 7.51 ppm. When compared to **H1**, the latter signal is shifted slightly upfield.

In addition, benzylic alcohols **19** and **20** (Chart 2) used as reference compounds in the optical studies were prepared by diisobutylaluminum hydrid (DIBAL-H) reduction of benzaldehydes **6** and **9**, respectively.

Optical Properties. H1 and H2. The electronic absorption spectra of **HX0**, **H1**, and **H2** in cyclohexane solution are depicted in Figure 3 (top left). The spectrum of the reference phenyeneacetylene (PA) **HX0** is very similar to an analogous trimer system lacking the peripheral triple bonds,[13] suggesting negligible increase of π-conjugation length. By connecting two **HX0** units via an *ortho* PA bridge, little band broadening is observed, with an absorption onset red-shift of only 17 nm (Table 1); this indicates negligible criss-cross electronic delocalization over the whole structure in **H1**. In other words, the conjugation is effective for the *para*-linked subunits but the *ortho*- and *meta*-linked ethynylbenzene moieties do not really increase the conjugation length of the system.

The fluorescence spectra of **HX0** and **H1** have practically the same shape and vibronic structure (Figure 3, top right), but the emission maximum of **H1** is red-shifted by 20 nm, in line with the absorption trend. The singlet

(13) Melinger, J. S.; Pan, Y. C.; Kleiman, V. D.; Peng, Z. H.; Davis, B. L.; McMorrow, D.; Lu, M. *J. Am. Chem. Soc.* **2002**, *124*, 12002.

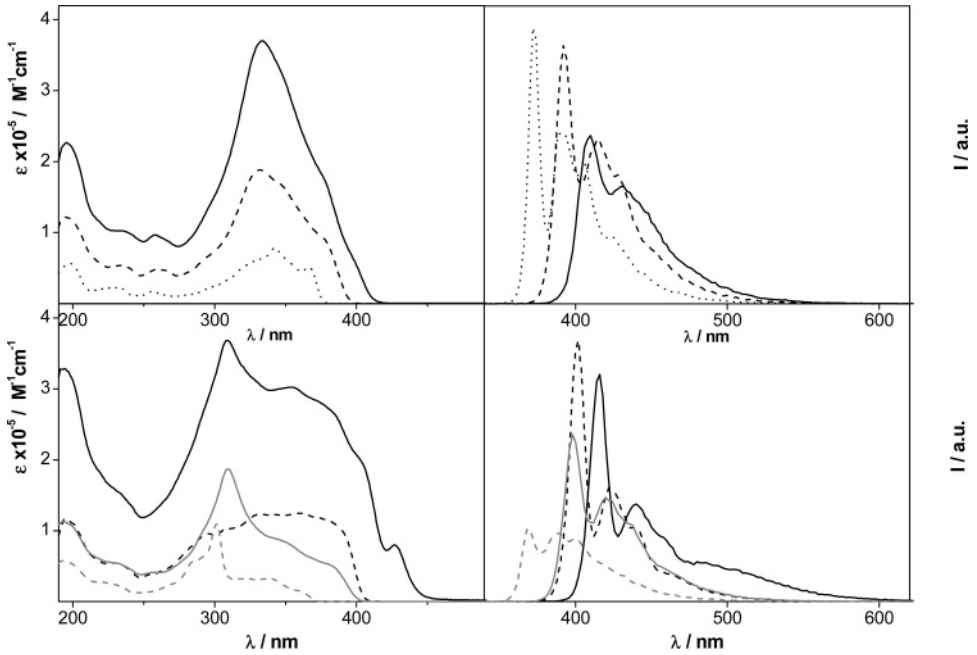

FIGURE 3. Top left: Absorption spectra of **HX0** (dotted line), **H1** (dashed line), and **H2** (full line) in cyclohexane. Top right: Emission spectra of isoabsorbing solutions ($A = 0.18$) of **HX0** (dotted line), **H1** (dashed line), and **H2** (full line) in cyclohexane. $\lambda_{ex} = 320$ nm. Bottom left: Absorption spectra of **X1** (dashed black line), **X2** (full black line), **19** (dashed gray line), and **20** (full gray line) in cyclohexane. Bottom right: Emission spectra of isoabsorbing solutions ($A = 0.18$) of **X1** (dashed black line), **X2** (full black line), **19** (dashed gray line), and **20** (full gray line) in cyclohexane. $\lambda_{ex} = 320$ nm.

TABLE 1. Optical Properties in Cyclohexane

	λ^{ab}_{max} (nm) [a]	λ^{ab}_{edge} (nm) [b]	ϵ_{max} (M^{-1} cm^{-1}) [c]	λ^{em}_{max} (nm) [d]	ϕ_{fl} [e]	τ (ns) [f]
HX0	342	377	7 850	372	1.00	0.6
H1	332	394	188 200	392	0.97	1.2
H2	334	408	370 000	410	0.89	2.4
X1	360	406	124 500	402	1.00	0.6
X2	309	442	368 500	416	0.61	0.7

[a] Maximum absorption wavelength. [b] Absorption onset corresponding to the wavelength at which ϵ is 5% of ϵ_{max}. [c] Molar extinction coefficient of the absorption maximum. [d] Fluorescence emission values obtained from uncorrected spectra. [e] Fluorescence quantum yield. [f] Singlet lifetimes from fluorescence decays.

excited state of **HX0** deactivates only via the radiative path ($\Phi_{fl} = 1.0$), whereas for **H1** some little nonradiative deactivation occurs ($\Phi_{fl} = 0.97$), probably as a consequence of the larger structure that favors vibrational deactivation. The radiative deactivation rate constant ($k_r = \Phi/\tau$) amounts to 1.7×10^9 and 8.3×10^8 s^{-1} for **HX0** and **H1**, respectively. **H2** is made of two **H1** units linked through a phenylacetylene spacer, but the electronic absorption spectrum is practically identical and twice as intense relative to that of **H1** for a large part of the spectrum (190−385 nm). Notably, the spectral onset of **H2** is slightly red-shifted compared to **H1**, and a weak absorption tail is observed down to 420 nm. These results suggest that, in the ground state, the two **H1**-type fragments of **H2** are substantially decoupled, but this does not prevent the occurrence of a lower-lying singlet state, as signaled by a red-shifted and longer lived fluorescence ($\lambda_{max} = 408$ nm, $\tau = 2.4$ ns, Table 1, Figure 3) relative to **H1**. The excitation spectra of **HX0**, **H1**, and **H2** in cyclohexane perfectly match the absorption profile at any emission wavelength and no evidence of molecular aggregation (e.g., excimer emission) is detected within the range of concentrations used for optical measurements ($10^{-5}/10^{-7}$ M).

X1 and X2. The electronic absorption spectra of **X1** and **X2** in cyclohexane solution are depicted in Figure 3 (bottom left). Such spectra are broad and poorly resolved (especially **X1**) and do not bear much resemblance to those of **19** and **20**, which may be considered the end units of **X1** and **X2**. This indicates that the electronic π-delocalization mainly occurs through the central molecular backbone made of five and seven *p*-phenylacetylene units for **X1** and **X2**, respectively; this pattern mainly dictates the absorption profile. The larger delocalization of the central molecular wire in **X2** leads to a 36 nm red-shift of the absorption onset relative to **X1**, and a 14 nm shift of the first feature of the fluorescence spectra (Figure 3, Table 1). The fluorescence quantum yield and the singlet excited-state lifetime of **X1** are identical to that of the reference system **HX0**. The excitation spectra of **X1** and **X2** in cyclohexane match the absorption profile at any emission wavelength. It is noteworthy to mention here that the lowest energy absorption peak observed in freshly prepared solutions of **X2** tends to decrease over time (minutes), this is attributed to some molecular aggregation of this large extended π-conjugated system.

It must be emphasized that **H1/X1** and **H2/X2** are isomer couples whose different electronic π-conjugation pattern is reflected in the differences of the absorption spectra (Figure 4). The **X**-type molecules exhibit a lower lying absorption onset and a wider spectral profile. The fluorescence yield is virtually unitary for **H1** and **X1**, whereas for **X2** a substantially lower value is found, compared to **H2** (Table 1). **X2** does not exhibit any detectable phosphorescence at 77 K.

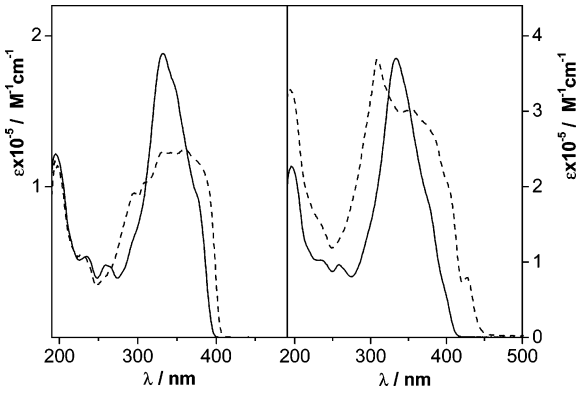

FIGURE 4. Left: absorption spectra of **H1** (full line) and **X1** (dashed line) isomers in cyclohexane. Right: absorption spectra of **H2** (full line) and **X2** (dashed line) isomers in cyclohexane.

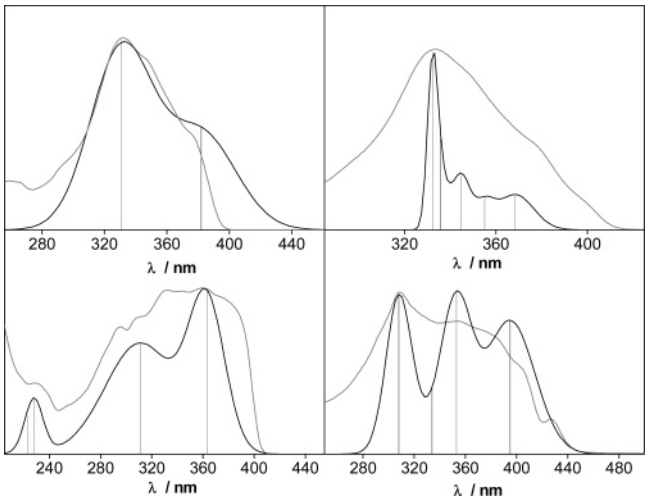

FIGURE 5. Measured (gray full line) and simulated absorption (black full line) spectra of **H1** (top left), **H2** (top right), **X1** (bottom left), and **X2** (bottom right). The calculated energies have been shifted in order to let the calculated and experimental spectra maxima coincide.

Analysis of Absorption Spectra. The absorption spectra of the main compounds examined in this work have been simulated using the oscillator strengths calculated with the ZINDO/S program[14] included in the Hyperchem package,[15] having previously optimized the ground-state geometry within the MM+ force field. The simulation was obtained using a Gaussian shape of the bands centered on the calculated wavelength and a semibandwidth of 30 nm, having shifted the computed energies so that the wavelengths of the experimental and calculated maxima coincide. The method used, despite its simplicity, provides a satisfactory description of the main features of the experimental spectra, as already underlined by comparison with more sophisticated methods employed in the study of analogous compounds.[16,17]

In particular, the spectra displayed in Figure 5 show a reasonable agreement for the band shape and calculated energies of the simpler compounds **H1** and **X1**, where the large absorption system detected in the region of 280−400 can be accounted for by two main transitions to S_1 (calculated at 406 and 399 nm, respectively) and S_2 (calculated at 355 and 346 nm). The calculated red shift of the **X1** bands with respect to those of **H1** can be fairly well accounted for by a larger conjugation shown by the former compound, with a wire of five phenylacetylene units versus three in the case of **H1**. Also the different shape of the absorption bands shown by the two classes of compounds (**H1**, **H2** versus **X1**, **X2**) can be explained by the different amount of π electron delocalization. In fact, the oscillator strength of the most intense band of **H1** (S_2), which is calculated to be about twice the amount of **X1** (S_1), can be explained by the sum of two separated wires made of three phenylacetylene units, due to the poor electronic conjugation brought about by the transversal bridge. This feature appears evident when inspecting the nature of the molecular orbitals involved in the transitions to these states and displayed in Figures 6 and 7. In **H1**, the very intense band calculated at 355 nm is largely due to the transition (HOMO − 1) → (LUMO + 1), showing a break of electron density in correspondence of the central phenyl of the bridge. On the other hand, the most intense calculated band of **X1** (S_1) arises essentially from the HOMO → LUMO transition, localized on the central wire made of five phenylacetylene units, with minor participation of the side branches.

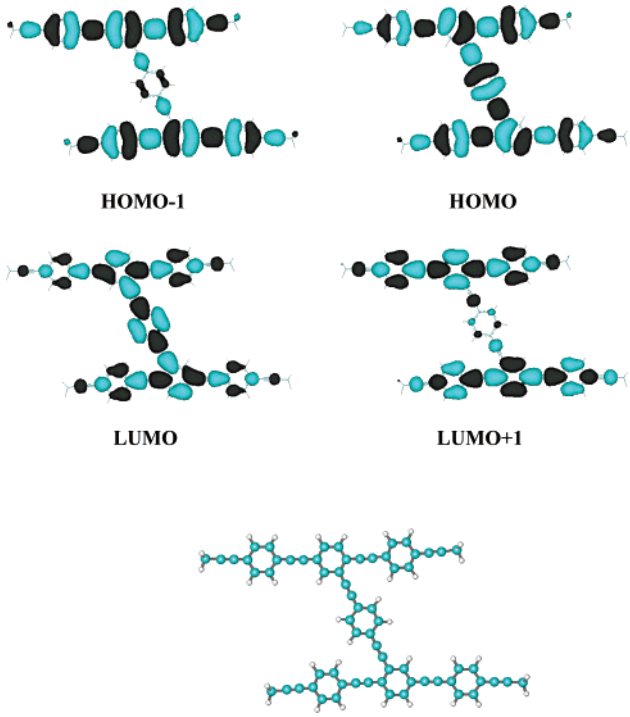

FIGURE 6. Calculated HOMO and LUMO Orbital Distributions for **H1** (dark gray negative, light-blue positive) and **H1** MM+ minimized structure.

Conclusion

We have developed an iterative approach for the preparation of new branched conjugated systems with a terminal alkyne function starting from 4-(triisopropylsilylethynyl) phenylacetylene (**4**) by applying the follow-

(14) Ridley, J.; Zerner, M. C. *Theor. Chim. Acta* **1973**, *32*, 111.
(15) *Hyperchem*, version 6.02; Hypercube Inc.: Gainesville, FL, 2000.
(16) Magyar, R. J.; Tretiak, S.; Gao, Y.; Wang, H.-L.; Shreve, A. P. *Chem. Phys. Lett.* **2005**, *401*, 149.
(17) Houk, K. N., Lee, P. S., Nendel, M. *J. Org. Chem.* **2001**, *66*, 5517.

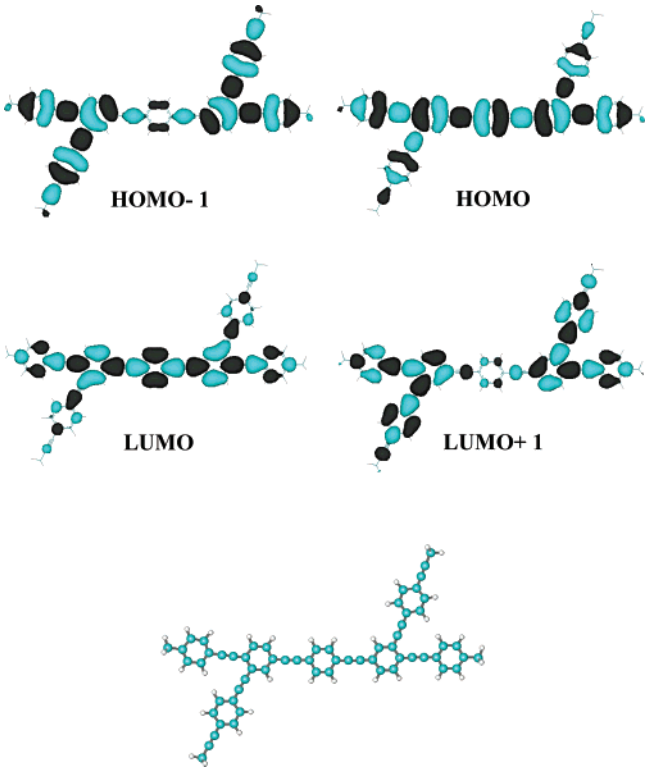

FIGURE 7. Calculated HOMO and LUMO Orbital Distributions for **X1** (light-blue negative, dark-grey positive) and **X1** MM+ minimized structure.

ing reaction sequence: (i) metal-catalyzed cross-coupling reaction of the terminal alkyne with a dibromobenzaldehyde derivative (**5** or **12**); (ii) Corey-Fuchs dibromoolefination and treatment with an excess of LDA.[12c] The building blocks thus prepared have been subjected to a Pd-catalyzed cross-coupling reaction with 1,4-diiodobenzene to yield the isomeric branched π-conjugated systems containing 7 (**H1** and **X1**) or 15 (**H2** and **X2**) phenyl units connected by ethynyl spacers. The different π-conjugation patterns in those isomeric derivatives have a dramatic effect on their electronic properties as attested by the differences observed in their absorption spectra. Finally, it can be added that all of these extended conjugated derivatives are highly luminescent with nearly quantitative fluorescence quantum yields. The results described in this paper provide a hint for the design of novel branched conjugated systems with tailored optical properties, and the characteristic features of these compounds make them attractive photoactive components for the preparation of photochemical molecular devices or new sensors. Work in this direction is now underway in our laboratories.

Experimental Section

General. Reagents and solvents were purchased as reagent grade and used without further purification. THF was distilled over sodium benzophenone ketyl. Compounds **5**[18] and **12**[19] were prepared as previously reported.

General Procedure for Dibromoolefination Reactions. A mixture of CBr_4, PPh_3, and Zn dust in dry CH_2Cl_2 was stirred at room temperature for 24 h. The suspension was then cooled to 0 °C, and the appropriate aldehyde dissolved in CH_2Cl_2 was added at once. The resulting mixture was slowly warmed to room temperature and stirred overnight. The resulting thick suspension was filtered and evaporated. The residue was dissolved in a minimum of CH_2Cl_2, and then hexane was added to precipitate the remaining P-containing byproducts. The resulting mixture was filtered and evaporated. The product was then purified as outlined in the following text.

Compound 3. This compound was prepared from **2** (6.77 g, 23.7 mmol), CBr_4 (39.9 g, 118.6 mmol), PPh_3 (31.1 g, 118.6 mmol), and Zn dust (7.75 g, 118.6 mmol) in CH_2Cl_2 (450 mL), and column chromatography (SiO_2, hexane) yielded **3** (10.48 g, 99%). Colorless oil. IR (CH_2Cl_2): 2288 (C≡C). ^{1}H NMR ($CDCl_3$, 200 MHz): δ 7.48 (s, 4H), 7.46 (s, 1H), 1.15 (s, 21 H). ^{13}C NMR ($CDCl_3$, 50 MHz): δ 136.0, 134.9, 131.9, 128.1, 123.6, 106.7, 92.1, 90.4, 18.7, 11.3. Anal. Calcd for $C_{19}H_{26}Br_2Si$: C 51.59, H 5.92. Found: C 51.51, H 6.01.

General Procedure for Preparation of Alkynes from Dibromoolefines. A solution of LDA in THF was slowly added to a solution of the appropriate dibromoolefine in THF at −78 °C. After 3 h, a saturated aqueous NH_4Cl solution was added. The reaction mixture was diluted with hexane, washed with water, dried with $MgSO_4$, and evaporated. The product was then purified as outlined in the following text.

Compound 4. This compound was prepared from **3** (14.09 g, 32.8 mmol) and LDA (134 mmol) in THF (450 mL), and column chromatography (SiO_2, hexane) yielded **4** (8.34 g, 90%). Colorless oil. IR (CH_2Cl_2): 3315 (≡C−H), 2152 (C≡C). ^{1}H NMR ($CDCl_3$, 200 MHz): δ 7.42 (s, 4H), 3.17 (s, 1H), 1.14 (s, 21 H). ^{13}C NMR ($CDCl_3$, 50 MHz): δ 131.8, 131.7, 123.9, 122.1, 106.5, 92.8, 83.2, 18.6, 11.3. Anal. Calcd for $C_{19}H_{26}Si$: C 80.78, H 9.28. Found: C 80.80, H 9.01.

General Procedure for Sonogashira Cross-Coupling Reactions. To an oven-dried glass screw capped tube were added all solids including the aryl halide (bromide or iodide), alkyne, CuI, PPh_3, and palladium catalyst. The atmosphere was removed via vacuum and replaced with dry argon (3×). THF and triethylamine were added by syringe, and the reaction was conducted at room temperature (for aryl iodides) or heated at 65 °C in an oil bath with stirring (for aryl bromides). Upon cooling the reaction mixture was filtered via gravity filtration to remove solids and diluted with dichloromethane. The reaction mixture was extracted with an aqueous NH_4Cl solution. The organic layer was dried with $MgSO_4$ and filtered through a plug of SiO_2 (CH_2Cl_2). The solvent was evaporated, and the product was purified as outlined in the following text.

Compound 2. This compound was prepared from triisopropylsilylacetylene (15 mL, 67 mmol), **1** (10.0 g, 54 mmol), $Pd(PPh_3)_2Cl_2$ (248 mg, 0.36 mmol), CuI (72 mg, 0.36 mmol), and PPh_3 (0.23 g, 0.88 mmol) in THF/Et_3N (100 mL). Column chromatography (SiO_2, hexane/CH_2Cl_2 2:1) yielded **2** (15.16 g, 98%). Colorless oil. IR (CH_2Cl_2): 2286 (C≡C), 1704 (C=O). ^{1}H NMR ($CDCl_3$, 200 MHz): δ 10.01 (s, 1H), 7.83 (d, J = 7 Hz, 2H), 7.62 (d, J = 7 Hz, 2H), 1.15 (s, 21H). Anal. Calcd for $C_{18}H_{26}SiO$: C 75.46, H 9.15. Found: C 75.62, H 9.26.

General Procedure for Reduction. A 1 M solution of DIBAL-H in hexane was slowly added to a solution of the appropriate benzaldehyde in THF at 0 °C under argon. After 3 h, methanol and then water were added. The reaction mixture was filtered through a pad of Celite, dried ($MgSO_4$), filtered, and evaporated. The product was then purified as outlined in the following text.

Compound 19. This compound was prepared from **6** (80 mg, 0.12 mmol) and DIBAL-H (0.5 mL, 0.5 mmol), in THF (5 mL). Column chromatography (SiO_2, hexane/CH_2Cl_2 1:4) yielded **19** (59 mg, 73%). Pale yellow solid (mp 124 °C). IR (KBr): 3300 (O−H), 2152 (C≡C). ^{1}H NMR (200 MHz, $CDCl_3$): δ 7.58 (broad s, 1H), 7.(d, J = 7 Hz, 1H), 7.48 (s, 8H), 7.33 (broad d, J = 7

(18) Swoboda, P.; Saf, R.; Hummel, K.; Hofer, F.; Czaputa, R. *Macromolecules* **1995**, *28*, 4255.
(19) Schweikart, K.-H.; Hanack, M.; Lüer, L.; Oelkrug, D. *Eur. J. Org. Chem.* **2001**, 293.

Hz, 1H), 4.73 (s, 2H), 1.15 (s, 42H). Anal. Calcd for $C_{45}H_{56}OSi_2$: C 80.78, H 8.44. Found: C 80.80, H 8.50.

Acknowledgment. This research was supported by CNRS, CNR (*commessa PM-P04-ISTM-C1/PM-P04-ISOF-M5, Componenti Molecolari e Supramolecolari o Macromolecolari con Proprietà Fotoniche ed Optoelettroniche*) the French Ministry of Research (*ACI Jeunes Chercheurs*), the Italian MIUR (contract FIRB RBNE-019H9K, Molecular Manipulation for Nanometric Machines) and the EU (RTN Contract "FAMOUS", HPRN-CT-2002-00171). S.Z. thanks the Direction de la Recherche of the French Ministry of Research, and A.G. thanks the ADEME-Région Alsace for their fellowships. We further thank L. Oswald for technical help and J.-M. Strub for MS measurements.

Supporting Information Available: ^1H and ^{13}C NMR spectra of compounds **6**−**11**, **13**−**18**, **X1**, **X2**, **H1** and **H2**; the computational data for **X1** and **H1**; and the experimental details for the preparation of compounds **6**−**11**, **13**−**18**, **HX0**, **X1**, **X2**, **H1**, **H2**, and **20**. This material is available free of charge via the Internet at http://pubs.acs.org.

JO0506581